© 2017 IJSRST | Volume 3 | Issue 7 | Print ISSN: 2395-6011 | Online ISSN: 2395-602X
Themed Section: Science and Technology

Intense Frequency Upconversion Emission of Rare Earth Codoped Lead Bismuth Gallium Borate Glasses

Krishna Murthy Goud K*1, Ramesh Ch2 and Appa Rao B3
*1Department of Physics, UCE (A), Osmania University, Hyderabad (T.S), India
2 Department of Physics, Mahatma Gandhi University, Nalgonda (T.S), India
3 Department of Physics, UCS, Osmania University, Hyderabad-500007 (T.S), India

ABSTRACT

In order to develop efficient upconversion laser materials in the visible region an active lead borate matrix codoped with Tm^{3+}/Yb^{3+} rare earth ions has been studied extensively. Optical absorption, DSC, FTIR and photoluminescence spectra of these glasses have been studied. Judd-Ofelt theory has been applied to the f ↔ f transitions for evaluating Ω_2, Ω_4 and Ω_6 parameters. Radiative properties like branching ratio β_r and the radiative life time τ_R have been determined on the basis Judd–Ofelt theory. Taking advantage of the high absorption transition probability of the Yb^{3+} ions, these ions are excited with 980 nm radiation from a commercial laser diode and subsequently de-excited by efficiently transferring energy to the Tm^{3+} ions. The spectra exhibited two emission bands centered at 468 nm and 654 nm due to $^1G_4 \rightarrow {}^3H_6$ and $^1G_4 \rightarrow {}^3H_4$ transitions, respectively. The results obtained are discussed quantitatively based on the energy transfer between Yb^{3+} and Tm^{3+}. Comparing the obtained values to those reported in other Tm^{3+}/Yb^{3+} doped materials, the lead bismuth gallium borate glasses doped with 0.2 mol% of Yb_2O_3 ions 0.6 mol% of Tm_2O_3 can be considered excellent candidates for developing blue upconversion laser materials in the visible region.

Keywords: DSC, FTIR, Optical absorption, Photo luminescence, Upconversion

I. INTRODUCTION

This With the development of up-conversion visible or ultraviolet photonic devices, rare earth ions-doped glasses have been investigated extensively, which may be the candidate materials to be applied in areas of high density optical storage, color displays, optoelectronics, upconversion laser materials and medical diagnostics [1–4]. Rare earth ions, such as Er^{3+} [5–7], Ho^{3+} [8, 9] and Tb^{3+} [10, 11], sensitized with ytterbium, have been widely studied in various host materials and their upconversion properties were researched for developing the glasses with the intense frequency upconversion emission. In certain situations, one takes advantage of the strong absorption cross-section of Yb^{3+} around 980 nm and the efficient energy transfer mechanism between Yb^{3+} ions and those rare earth acceptors. For a lot of applications, it is desirable to access the visible wavelength emitting levels of such rare earth (RE) ions employing an excitation source in the wavelength region of 980 nm [12].

In previous researches, Tm^{3+}/Yb^{3+} codoped fluoride and tellurite glasses were investigated under 980 nm laser diode (LD) excitation and were shown to be effective blue luminescence materials through the Tm^{3+}:$^1G_4 \rightarrow {}^3H_6$ transition [13, 14]. In this work, we report for the first time the spectral properties of Yb^{3+}/Tm^{3+} codoped lead bismuth gallium borate glasses. The XRD, optical absorption, FTIR and up-conversion under 980 nm excitation have been measured and the results are discussed finally.

II. EXPERIMENTAL METHODS

An For the present study, glasses with the composition $[100-(x+y)][0.5PbO-0.25B_2O_3-0.20Bi_2O_3-0.05Ga_2O_3]-xTm_2O_3-yYb_2O_3$ with $y = 0$ for $x = 0, 0.2$ and $y = 0.2$ for $x = 0$ to 1.0 (step 0.2 mol%) are chosen and the glass samples are labelled as G1, G2, G3, G4, G5, G6, G7 and G8 respectively. Appropriate amounts of AR grade reagents of PbO, B_2O_3, Bi_2O_3, Ga_2O_3, Tm_2O_3 and Yb_2O_3 powders were weighed by using digital electronic balance. These chemicals were mixed and thoroughly ground in a mortar to get a homogeneous mixture and melted in a porcelain crucible in the temperature range of 900 to 950 ^{o}C in a programmable electrical furnace for thirty minutes until bubble free liquid is formed. The resultant melt is poured in a brass mould and subsequently annealed at 300 ^{o}C for about four hours in order to avoid these internal mechanical stresses. After annealing, both surfaces of the samples were optically polished to the dimensions of 1 cm × 1 cm × 0.2 cm in order to meet the requirements for optical measurements. The structure of the samples was tested by means of X-ray diffraction using Rigaku miniflex table top X-ray diffractometer with Cu Kα radiation at room temperature. The diffractograms have been measured in the range of 10°- 80° with a scanning speed of 2.4°/min. The optical absorption spectra were obtained with the JASCO Model V-670 UV–VIS–NIR spectrophotometer in the wavelength range 350–1600 nm with a spectral resolution of 0.1 nm. The FTIR spectra of glass samples were recorded on a BRUKER OPTICS, TENSOR-27 infrared spectrometer in the range 4000 – 400 cm^{-1}. These measurements were made on glass powder dispersed in KBr pellets. The visible upconversion fluorescence spectra were recorded using JOBIN YVON Fluorolog-3 spectrofluorimeter in the wavelength range 300-700 nm under the excitation of 980 nm laser diode.

III. RESULTS AND DISCUSSION

A. Physical Parameters

Densities were measured according to Archimedes's principle. The molar volume (V_m) of the samples was calculated using the values of density (ρ) and average molecular weight (M). The calculated values of density (ρ) and molar volume (V_m) of the glass samples are presented in Table 1.

It was observed that molar volume decreases monotonically with the increase of Tm_2O_3 concentration, which indicates that the topology of the network is significantly changed with composition. On the other hand, these trends can be explained rather simply due to the replacement of a lighter cation (B) by a heavier one (Tm) [15]. From the measured values of the density and average molecular weight M of the samples, various other physical parameters such as molar volume, oxygen packing density, Tm^{3+} and Yb^{3+} ion concentration N_i, mean Tm^{3+} and Yb^{3+} ion separation r_i and polaron radius r_p were computed using standard equations [16] and are presented in Table 1.

B. X-Ray Diffraction

Title The X-ray diffraction (XRD) spectra for all the glass samples were recorded using Rigaku miniflex table top X-ray diffractometer with Cu Kα radiation at room temperature. The X-ray diffraction spectra of all the samples is shown in Fig. 1.

The samples prepared were free from visible inhomogeneities, such as inclusions, cracks or bubbles. Based upon the visual examination, the absence of peaks in the X-ray diffraction pattern, the existence of glass transition temperature (T_g), we could come to the conclusion that the samples prepared were of amorphous in nature.

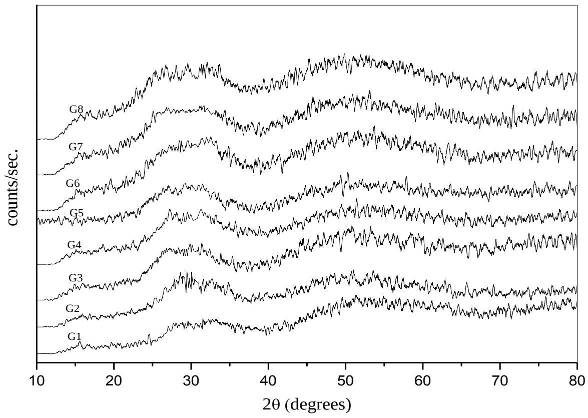

Figure 1. XRD spectra of Tm^{3+}/Yb^{3+}codoped lead bismuth gallium borage glasses.

C. Differential Scanning Calorimetry

The DSC thermograms were recorded using DSC Q20 (TA-Instruments) with a programmed heating rate of 20°C per minute in the temperature range 50-450°C and presented in the Fig. 2.

Figure 2 shows typical differential thermal analysis thermograms of the glasses under investigation. These thermograms are characterised by an endothermic change between 360 and 390°C corresponding to the glass transition temperature Tg. The appearance of a single peak corresponding to Tg for each glass indicates that the prepared glasses are of highly homogenous. The glass transition temperatures of all the glass samples were determined by differential scanning calorimetry traces and were presented in Table 2.

TABLE I

VARIOUS PHYSICAL PARAMETERS OF THE RARE EARTH CODOPED LEAD BISMUTH GALLIUM BORAGE GLASSES

Physical parameter	**G1**	**G2**	**G3**	**G4**	**G5**	**G6**	**G7**	**G8**
Avg. molecular weight, M(g/mol)	232.56	232.96	232.86	233.18	233.51	233.81	234.13	234.47
Density, ρ(g/cm^3) (±0.001)	6.508	6.588	6.545	6.618	6.690	6.763	6.836	6.906
Oxygen packing density, O (g atom/L)	0.0567	0.0573	0.0570	0.0574	0.058	0.0586	0.0592	0.0597
Tm ion concentaration, N_i (x10^{21}/cm^3) (±0.001)	-	-	0.106	0.106	0.212	0.322	0.432	0.536
Molar Volume, V_m(cm^3/mol) (±0.01)	34.98	34.67	34.87	34.55	34.22	33.90	33.58	33.27
Tm Inter ionic distance, r_i (Å) (±0.01)	-	-	21.37	21.37	16.81	14.74	13.40	12.41
Polaran radius of Tm, r_p (Å) (±0.01)	-	-	12.68	12.68	9.72	8.42	7.56	6.95
Yb ion concentaration, N_i (x10^{21}/cm^3) (±0.001)	-	0.103	-	0.103	0.103	0.103	0.103	0.103
Yb Inter ionic distance, r_i (Å) (±0.01)	-	21.33	-	21.33	21.33	21.33	21.33	21.33
Polaran radius of Yb, r_p (Å) (±0.01)	-	12.65	-	12.65	12.65	12.65	12.65	12.65

The glass transition temperature values shows decreasing trend with increase in the concentration of Tm^{3+} ions up to 0.6 mol% (G6). The decreasing nature of the glass transition temperature up to G6 indicates, an increasing concentration of Ga^{3+} ions that take part network modifying positions. Beyond this concentration range (G6), the value of the glass transition temperature T_g has been observed to increase, due to the augmented cross-link density of various structural groups and closeness of packing are responsible for such increase of glass transition temperature. This result apparently indicates that, Ga^{3+} ions mostly occupy network-forming positions, increase the crosslink density and enhance the mean bond strength.

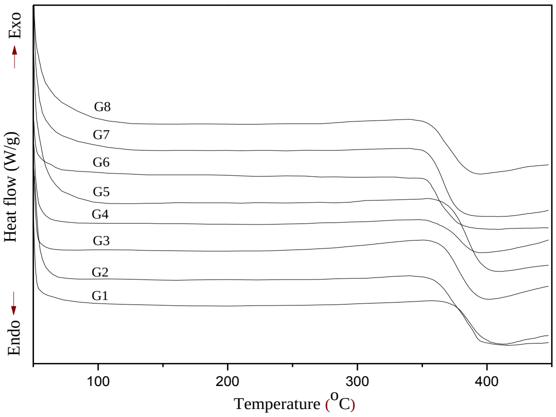

Figure 2. DSC thermograms of Tm^{3+}/Yb^{3+}codoped lead bismuth gallium borage glasses.

D. Optical Absorption

Place The optical absorption spectra of GTY glasses were obtained with the JASCO Model V-670 UV–VIS–NIR spectrophotometer in the wavelength range 400–2000 nm with a spectral resolution of 0.1 nm. Figure 3 shows optical absorption spectra of all prepared glass samples. The spectra exhibited an absorption band at 980 nm due to $^2F_{7/2} \rightarrow {}^2F_{5/2}$ transition of Yb^{3+} ions. The other absorption bands at 656 nm ($^3H_6 \rightarrow {}^3F_2$), 690 nm ($^3H_6 \rightarrow {}^3F_3$), 788 nm ($^3H_6 \rightarrow {}^3H_4$), 1215 nm ($^3H_6 \rightarrow {}^3H_5$) and 1655 nm ($^3H_6 \rightarrow {}^3F_4$) are attributed to 4f-4f transitions of Tm^{3+} ions, respectively [17-19].

Assignments to the various observed bands made by comparing their band positions with the previously reported transitions of Tm^{3+} ions in other glass systems. The intensities of all absorption bands attributed to Tm^{3+} were found to increase with increase in the concentration of Tm^{3+} ions and no significant shift is observed in the band positions. From the spectra it was observed that cut-off wavelength value increases upto 0.6 mol% (G6) of Tm^{3+} ions and decreases further with increase in the concentration of Tm^{3+} ions.

Urbach energy that is generally interpreted as the width of tail of energy levels in the optical energy gap and is found to increase with temperature. Highly crystalline solids show a very sharp absorption edge with small ΔE values. Therefore, Urbach energy can be considered as a measure of disorder in amorphous and crystalline materials [20-22]. The nature of disorder can be different in crystalline and amorphous solids. The disorder can be both static and dynamic. Dynamic disorder arises due to electron–phonon coupling in crystalline solids. In amorphous solids the static atomic structural disorder dominates and can be due to presence of defects like dangling bonds or non-bridging oxygens in glasses [23]. The UV–visible light absorption in oxide glasses is due to the excitation of electrons associated with NBOs [24]. The higher the concentration of NBOs in the glass network, the smaller the optical energy gap and the greater are the Urbach energy values in borate glasses [25].

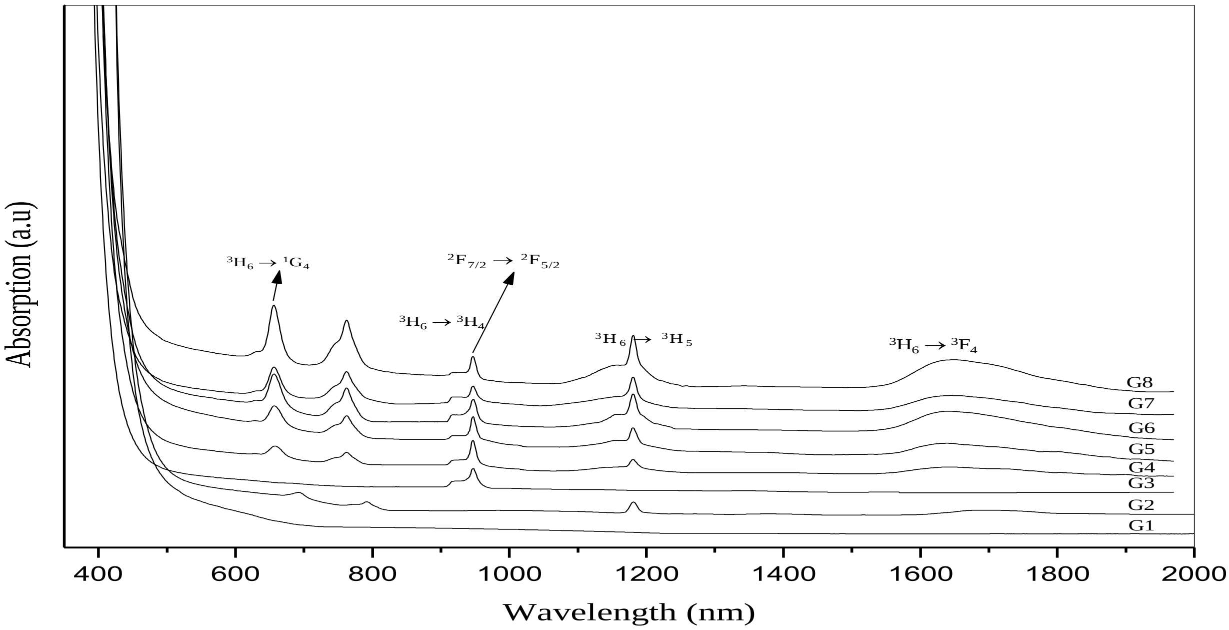

Figure 3. Optical absorption spectra of Tm^{3+}/Yb^{3+}codoped lead bismuth gallium borage glasses.

From the data (Table 2) it was observed that the decrease of optical band gap (E_{opt}), T_g and increase in Urbach energy takes place upto 0.6 mol% (G6) of Tm^{3+} ions. Further with increasing the concentration of Tm^{3+} ions the trend is reverse. The shift of optical absorption edge towards higher wavelength side and decrease in the optical band gap upto 0.6 mol% (G6) of Tm^{3+} ions is associated with increasing degree of depolymerization or concentration of bonding defects and concentration of triangular boron units containing non-bridging oxygens (NBOs), consistent with the observed decrease in T_g over this range.

TABLE III. VALUES OF CUT OFF WAVELENGTH, OPTICAL BAND GAP, TG AND URBACH ENERGY OF THE PRESENT GLASS SYSTEM

S.No.	**Sample code**	**Cut-off wavelength (nm)**	**E_{opt} (eV) ±0.01**	**ΔE (eV) ±0.001**	**T_g (°C)**
1	G1	417	3.08	0.144	388
2	G2	422	3.05	0.147	379
3	G3	425	3.03	0.150	378
4	G4	432	3.01	0.152	377
5	G5	437	2.99	0.156	370
6	G6	452	2.97	0.161	361
7	G7	448	3.00	0.155	363
8	G8	443	3.03	0.149	370

The increase in Urbach energy is indicative of an increase in concentration of NBOs and disorder in the glass network. As a modifier, Ga^{3+} ions increase the concentration of non-bridging oxygens (NBOs) by creating dangling bonds. Such defects increase the degree of localization of electrons, thereby increasing the donor centers in the glass matrix. The presence of large concentration of these donor centers lowers the optical band gap and shifts the absorption edge towards high wavelength side as observed. Probably in this concentration range the gallium ions may take network forming positions with GaO_4 structural units and alternate with BO_4 units. Such linkages may cause a decrease in the rigidity of the glass network and leads to the decrease in the optical band gap as observed.

J-O analysis

The Judd-Ofelt theory helps in the analyzation of the radiative transitions within in the $4f^{N}$ configuration of a rare earth ion. The Judd-Ofelt parameters Ω_2, Ω_4, Ω_6 and experimental (f_{exp}) and calculated (f_{cal}) oscillator strength values, radiative life time (τ_R) and branching ratio (β_r) were calculated using the J-O analysis. The results are summarized in Table 3 and Table 4.

The values of Judd-Ofelt intensity parameters are found to be $\Omega_2 = 1.98\text{x}10^{-20}$ cm^2, $\Omega_4 = 1.30\text{x}10^{-20}$ cm^2 and $\Omega_6 = 1.36\text{x}10^{-20}$cm^2, respectively. The values of Ω_λ are found to be in the following order: $\Omega_2 > \Omega_6 > \Omega_4$. The comparison of the data on Ω_λ parameters of Tm^{3+} ions in various other glass matrices indicated the same trend. The comparison of Judd-Ofelt parameters Ω_2, Ω_4 and Ω_6 of Tm^{3+} in various glass hosts is presented in Table 5.

TABLE IIII

EXPERIMENTAL AND CALCULATED OSCILLATOR STRENGTH OF TM^{3+} IN THE PRESENT GLASS SYSTEM

Transition	**Wavelength (nm)**	**Energy (cm^{-1})**	f_{exp}	f_{cal}
$^3H_6 \rightarrow {}^3F_2$	656	15244	7.284	7.561
$^3H_6 \rightarrow {}^3F_3$	686	14577	6.981	7.115
$^3H_6 \rightarrow {}^3H_4$	792	12626	5.684	5.578
$^3H_6 \rightarrow {}^3H_5$	1211	8257	3.451	3.598
$^3H_6 \rightarrow {}^3F_4$	1663	6013	3.987	4.102
rms deviation			±0.281	

TABLE IVV

RADIATIVE LIFE TIME (T_R) AND BRANCHING RATIOS (B_R) OF TM^{3+} IN THE PRESENT GLASS SYSTEM

Transitions	β_r **(%)**	τ_R**(ms)**
$^1G_4 \rightarrow {}^3H_6$	68.11	0.121
$^1G_4 \rightarrow {}^3H_4$	22.34	0.186

When a rare-earth ion is embedded in a glassy matrix (oxide or fluoride) strong covalent bond will exist between the rare-earth ion and the surrounding oxygen. The amount of covalency between these bonds can be inferred from the intensity and nature of hypersensitive transitions. Generally, the Ω_2, parameter is sensitive to the symmetry of the rare-earth site and strongly affected by covalency between rare-earth ions and ligand anions, whereas Ω_4 and Ω_6 are related to the rigidity of the host medium in which the ions are situated. It is widely accepted that Ω_4/Ω_6 determines the spectroscopy quality of the host materials [26, 27].

TABLE V

EXPERIMENTAL COMPARISION OF $\Omega_\lambda \times 10^{-20}$ (CM^{-2}) PARAMETERS FOR A NUMBER OF OTHER GLASS SYSTEMS CONTAINING TM^{3+} IONS

Glass system	Ω_2	Ω_4	Ω_6	**Reference**	Ω_4/Ω_6
Present glass system	1.98	1.30	1.36	Present work	0.96
Fluoro phosphate glass system	1.38	0.75	0.92	[35]	0.81
Antimony borate glass system	4.65	1.24	1.32	[37]	0.93

From Table 5, the present glass has a relatively low Ω_4/Ω_6 value than silicate, tellurite and fluoride glass system and is having high Ω_4/Ω_6 value than fluoro phosphate and antimony borate glass systems. The J–O parameters Ω_2 and Ω_4 are dominant for $^1G_4 \rightarrow {}^3H_6$ transition which is a possible laser transition of Tm^{3+} ion blue region [28]. The line strength of the $^3H_6 \rightarrow {}^3F_{2,3}$ transition which is in general used as the pumping level for blue upconversion emission from the $^1G_4$ level is dependent on Ω_6. From Table 4, branching ratio 'β_r' of the blue emission due to $^1G_4 \rightarrow 3H_6$ transition is found to be >50 %. The highest value of 'β_r' obtained for the present glass for the transition $^1G_4 \rightarrow {}^3H_6$ suggests that this glass is more preferable to produce high luminescence efficiency.

E. Fourier Transform Infrared Spectroscopy

The FTIR spectra of glass samples were recorded on a BRUKER OPTICS, TENSOR-27 infrared spectrometer in the range 4000 – 400 cm^{-1}. For IR measurements, the glasses were pulverized and mixed with KBr in order to obtain thin pellets with a thickness of about 0.3mm. Figure 4 shows the FTIR spectra of lead bismuth gallium borate glasses doped with rare earth ions in the range 1600-400 cm^{-1}. The FTIR spectra of lead bismuth gallium borate glass system shows characteristic bands corresponding to the different vibration modes of the various functional groups present in the glass system.

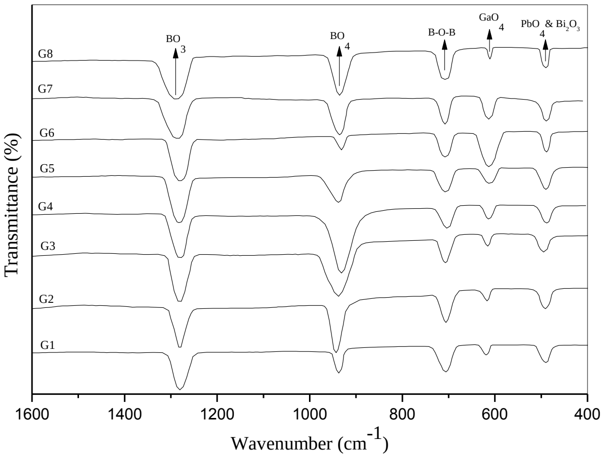

Figure 4. FTIR spectra of Tm^{3+}/Yb^{3+}codoped lead bismuth gallium borage glasses.

A band cited in the region ~490 cm^{-1} is identified due to bending vibrations of Bi_2O_3 pyramidal units and also due to the presence of PbO_4 structural units [29]. A band cited in the region ~610 cm^{-1} is identified due to network forming GaO_4 tetrahedral groups [30]. The band cited at ~707 cm^{-1} and is attributed to the vibrations of B-O-B linkages. A band cited in the region ~930 cm^{-1} is assigned to symmetric stretching vibrations of B-O bands in BO_4 units. The band cited in the region ~1280 cm^{-1} is identified due to asymmetric stretching modes of borate triangles BO_3 and BO_2O^-. The band positions and corresponding IR assignments were presented in Table 6.

PbO in addition to participating in the glass network with PbO_4 structural units, it may also enter as modifier. Ga_2O_3 is considered to act as a network former if Ga^{3+} ions take preferentially fourfold coordination in oxide glasses. The excess negative charge on GaO_4 tetrahedra is compensated either by localization of a modifier ion nearby or by generation of threefold oxygens. The GaO_4 tetrahedrons may enter the glass network and alternate with BO_4 tetrahedrons. In some of the glass networks, the gallium ions are also found to be in modifier positions with GaO_6 structural units [31]. From the spectra it was observed that intensity of band corresponding to GaO_4 tetrahedral groups increases from 0 mol% of Tm^{3+} ions (G1) to 0.6 mol% of Tm^{3+} ions (G6), beyond this concentration the trend is reverse. This is due to the fact that Ga^{3+} ions go into substitutional positions with GaO_4 structural units and alter the glass network upto 0.6 mol%. Within this concentration Ga^{3+} ions, isolate the rare-earth ions from RE-O-RE bonds and form Ga-O-RE bonds. Such declustering effect leads to the larger spacing between RE ions and may contributes for the enhancement of fluorescence emission.

TABLE VV

ABSORPTION BANDS AND THEIR ASSIGNMENTS FOR FT-IR SPECTRA

Wave number (cm^{-1})	**IR assignments**
~487	Bending vibrations of Bi_2O_3 pyramidal units, PbO_4 bending vibrations.
~616	Due to network forming GaO_4 tetrahedral groups.
~710	Vibrations of B-O-B linkages.
~937	Asymmetric stretching vibrations of B-O bands in BO_4 units.
~1265	Asymmetric stretching modes of borate triangles BO_3 and BO_2O^-.

F. Photo Luminescence

The visible upconversion fluorescence spectra were recorded using JOBIN YVON Fluorolog-3 spectrofluorimeter in the wavelength range 300-700 nm under the excitation of 980 nm laser diode. Figure 5 represents the upconversion emission spectra of Tm^{3+}/Yb^{3+} codoped lead bismuth gallium borate glass system in the wavelength range of 500 –700 nm under the excitation of 980 nm laser diode at room temperature. The spectra exhibited two emission bands centered at 468 nm and 654 nm due to $^1G_4 \rightarrow {}^3H_6$ (blue) and $^1G_4 \rightarrow {}^3H_4$ (red) transitions, respectively [32, 33].

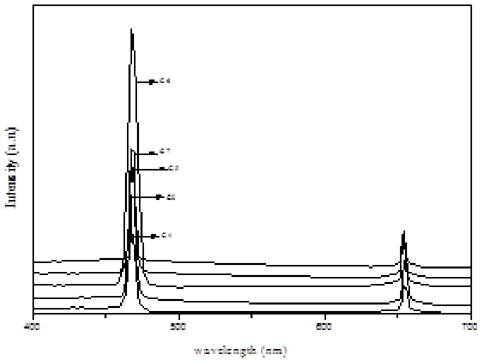

Figure 5. Frequency upconversion emission spectra of Tm^{3+}/Yb^{3+}codoped lead bismuth gallium borage glasses.

From the spectra it was observed that the upconversion luminescence intensity of blue emission (468 nm) is higher than the upconversion luminescence intensity of red emission (654 nm). It is also important to point out that the red emission is very weak and blue emission is very prominent to be observed by the naked eye at low excitation power for Tm^{3+}/Yb^{3+} codoped lead bismuth gallium borate glass system at room temperature. From the spectra it can be concluded that the intensity of blue and red emissions increases with increase in the concentration of Tm^{3+} ions upto 0.6 mol% (G6) and decreases with further increase in the concentarion of Tm^{3+} ions in Tm^{3+}/Yb^{3+} codoped glass samples. In an upconversion, the upconversion emission intensity (I_{up}) increases in proportion to the nth power of infrared excitation intensity (I_{IR}), i.e.,

$$I_{up}\,\alpha\, I_{IR}^{n}$$

where n is the number of IR photons absorbed per visible photon emitted [34]. A plot of log Iup versus log IIR yields a straight line with slope 'n'. From Fig. 6 (a) and (b) the slope value (n) for the 468 nm and 654 nm emission bands was calculated and got around three.

The results shows that a three photon upconversion process is responsible for the blue and red emissions from $^1G_4 \rightarrow {}^3H_6$ and $^1G_4 \rightarrow {}^3H_4$ transitions, respectively. Figure 7 represents the energy transfer mechanism between Yb^{3+} andTm^{3+} ions. The excitation process for the $^1G_4 \rightarrow {}^3H_6$ and $^1G_4 \rightarrow {}^3H_4$ transitions can be explained as follows. First Yb^{3+} ions in the ground level absorbs a photon and excites to the higher level ($^2F_{7/2} \rightarrow {}^2F_{5/2}$) then Yb^{3+} transfers their energy to the Tm^{3+} ions which are in ground level ($^3H_6$). This step is involved by energy transfer (ET) mechanism of excited Yb^{3+} to Tm^{3+}: (Yb) $^2F_{5/2}$ + (Tm) $^3H_6 \rightarrow$ (Yb) $^2F_{7/2}$ + (Tm) $^3H_5$. Actually the energy gap between (Yb) $^2F_{5/2}$ and (Yb) $^2F_{7/2}$ is in a wide range and the low energy edge is near the high energy edge of the energy gap between (Tm) $^3H_6$ and (Tm) $^3H_5$. Thus the energy transfer from Yb^{3+} becomes efficient [35].

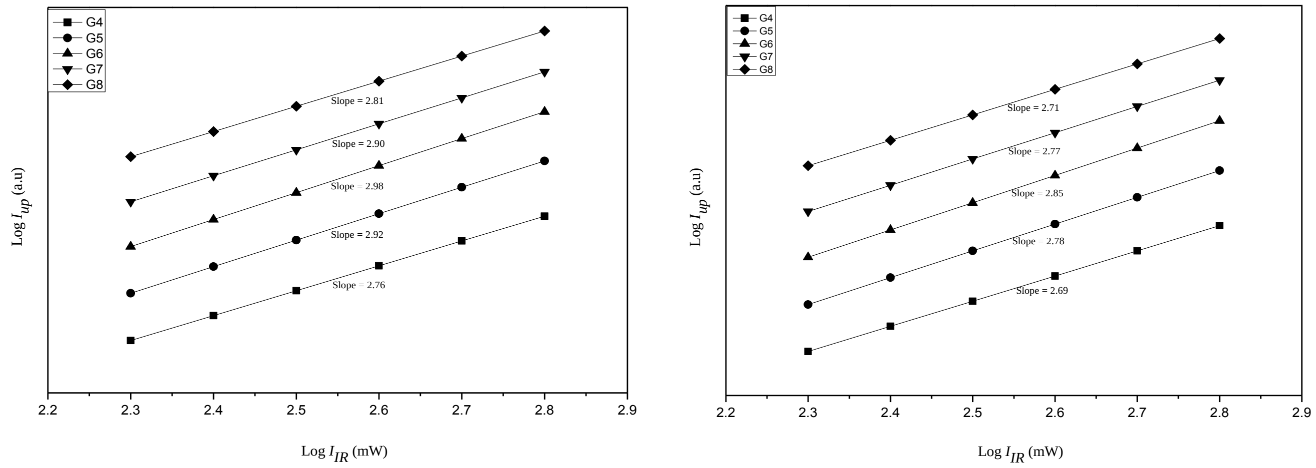

(a) (b)

Figure 6 (a). Dependence of upconversion fluorescence intensity of green emission (468 nm) on excitation power under 980 nm excitation. (b) Dependence of upconversion fluorescence intensity of red emission (654 nm) on excitation power under 980 nm excitation.

In the second step, Tm^{3+} in the ($^3H_5$) excited state relaxes nonradiatively to the metastable level ($^3H_4$) by the cooperation of the phonons in the alumina lead borate glasses. Tm^{3+} in the $^3H_4$ level is excited to $^3F_{2,3}$ level by ET from Yb^{3+} and absorption a photon. Thus, the population of $^3F_{2,3}$ level is based on the processes as follows: ET from Yb^{3+} : (Yb) $^2F_{5/2}$ + (Tm) $^3H_4 \rightarrow$ (Yb) $^2F_{7/2}$ + (Tm)^3 $F_{2,3}$ and excited state absorption (ESA): (Tm) $^3H_4$ + a photon → (Tm) $^3F_{2,3}$. Then the $^3F_{2,3}$ states also relaxes by a multiphonon assisted process to the $^3F_4$ level [36]. Finally, Tm^{3+} in the $^3F_4$ level is excited to $^1G_4$ level by ET from Yb^{3+} and absorption a photon. Therefore, the population of $^1G_4$ is based on the processes as follows: ET from Yb^{3+}: (Yb) $^2F_{5/2}$ + (Tm) $^3F_4 \rightarrow$ (Yb) $^2F_{7/2}$ + (Tm) $^1G_4$ and ESA: (Tm) $^3F_4$ + a photon → (Tm) $^1G_4$.

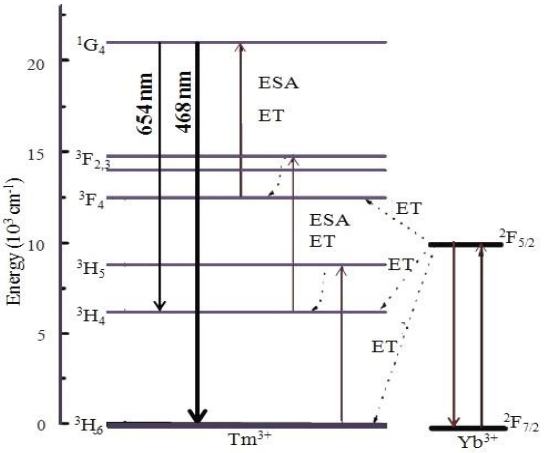

Figure 7. Energy transfer mechanism between Yb^{3+} andTm^{3+} ions.

It might be ascribed to the fact that the relaxations of $^3H_5$ to $^3H_4$ and $^3F_{2,3}$ to $^3F_4$ need the assistance of multiphonon relaxation, and the density of high energy phonon states is comparatively low in this glass. From the $^1G_4$ level, the Tm^{3+} ions decay radiatively to the $^3H_6$ ground state, generating the intense blue emission around 468 nm. This is a process that involved three photons. So the 468 nm emission presents nearly a cubic dependence on the excitation power. Though the phonon energy of the matrix is about 1000 cm^{-1}, the blue luminescence of Tm^{3+}/Yb^{3+} codoped samples can be seen by naked eye under excitation power as low as 70 mW. The red emission around 654 nm is due to the radiative decay of Tm^{3+} ions from the $^1G_4$ level to the $^3H_4$ level. The major contribution to the blue emission is ascribed to the $^1G_4 \rightarrow {}^3H_6$ transition. The transition probability involved in the blue emission process is very high compared to red emission process. Hence the observed red emission is weak.

From the above results it can be concluded that Tm^{3+} and Yb^{3+} showed a dominating role in the energy absorption and energy transfer in visible region. Because three photon upconversion fluorescence is more sensitive to pump energy. Intense blue emission has been observed when the excitation power rise to the value above 70 mW. It proven that commercial 980 nm laser diode is a power full pumping source for upconversion fluorescence in Tm^{3+}/Yb^{3+} codoped alumina lead borate glasses. Moreover, as mentioned before, the phonon energy also plays an important role and it can affect the upconversion intensity: with the increase of the phonon energy in Tm^{3+}/Yb^{3+} co-doped glasses the blue emission increases more than the red by means of the process described above.

Figure 8 represents the intensity of blue emission as a function of Tm_2O_3 at fixed Yb_2O_3 concentration in lead bismuth gallium borate glass system. From the figure it was observed that as the concentration of Tm_2O_3 is increased the blue emission band is observed to grow gradually up to 0.6 mol% and decreases further increasing the concentration of Tm_2O_3. A similar behavior is also observed in cut-off wavelengths of these glasses. This is due to the fact that Ga^{3+} ions (like any other III A group elemental ions), isolate the rare-earth ions from RE-O-RE bonds and form Ga-O-RE bonds. Such declustering effect which seems to be dominant in the glasses containing higher concentrations of Tm_2O_3, leads to the larger spacing between RE ions and contributes for the enhancement of fluorescence emission. Above 0.6 mol% of Tm2O3 there is a decrease in the emission intensity which may be due to concentration quenching.

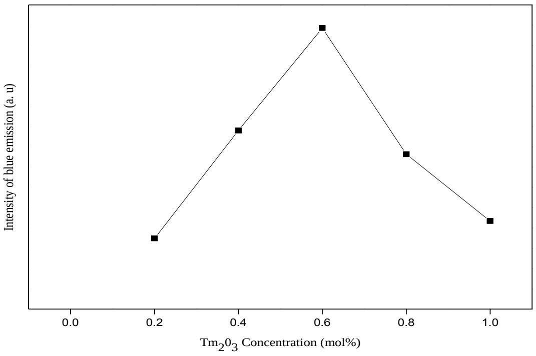

Figure 8. Intensity of blue emission as a function of Tm_2O_3 concentration with fixed Yb_2O_3 concentration in the present glass system.

The concentration quenching of auxiliary ions (Tm^{3+}) results from electron transfer among traps by tunneling. The average distance between an empty trap/erbium to a nearby charged trap will be reduced at higher Tm^{3+} concentrations. Therefore the probability of tunneling increases and the trapped electrons can easily reach quenching sites even at room temperature. Phonons may play a role in these processes [37-39]. This effect will not occur at low concentrations because then the average distance barrier width is too large. Codoping Tm^{3+} into the host lattice will result in complicated defects. Some kinds of these defects may act as quenching sites. As a result of such causes, the probability o non-radiative transitions of the luminescent molecules from the excited state to the ground state increases in comparison with the probability of radiative transitions. This will reduce the intensity of luminescence emission.

For the Yb^{3+}/Tm^{3+} codoped glass, the 480 nm blue luminescence can be quenched by the following process: Tm^{3+}: $^1G_4$+Tm^{3+}: $^3H_6$→Tm^{3+}: $^3H_4$+Tm^{3+}: $^3H_5$. However, when the concentration of Tm^{3+} ions is not too high, this quenching process is not notable because the 3H4 and 3H5 energy levels are still the interim states for the blue upconversion emission. Tm^{3+} ions in $^3F_4$ or $^3H_4$ can be sensitized again to $^1G_4$. It is just like a cycle. However, when the concentration of Tm^{3+} ions increases $^3F_4$ and $^3H_4$ states are depopulated by the energy transfer and the cycle breaks. Hence, luminescence quenching takes place resulting the decrease in the upconversion intensity.

IV.CONCLUSION

In summary, lead bismuth gallium borate glasses were prepared with different dopant (Tm^{3+}/Yb^{3+}) ion concentrations for the investigation of spectroscopic properties at room temperature. The absorption spectra and Judd–Ofelt analyses evidence the incorporation of rare earth ions in lead bismuth gallium borate glasses. The Judd–Ofelt intensity parameters Ω_t (t=2, 4, 6), oscillator strengths, branching ratios (β_r), and the radiative lifetimes were calculated and analyzed based on the absorption spectrum. From the values of branching ratio it was found that the transition $^1G_4 \rightarrow {}^3H_6$ (468 nm) has the highest value of β_r among various transitions. This transition may therefore be considered as a possible laser transition.

The upconversion bands centered at 468 nm and 654 nm corresponding to the $^1G_4 \rightarrow {}^3H_6$ and $^1G_4 \rightarrow {}^3H_4$ transitions of Tm^{3+}, respectively, were simultaneously observed at room temperature. The possible upconversion processes and mechanisms were mainly to involve the excited state absorption and the energy transfer. The energy transfer efficiency increases with Tm^{3+} content, and reaches maximum for the 0.6 mol% Tm^{3+}/0.2 mol% Yb^{3+} co-doped glass. From the upconversion spectra it was found that, the blue emission is more influenced than the red emission. The red emission around 654 nm is due to the radiative decay of Tm^{3+} ions from the $^1G_4$ level to the $^3H_4$ level. The major contribution to the blue emission is ascribed to the $^1G_4 \rightarrow {}^3H_6$ transition. The upconversion processes involved a three photon absorption for the blue and red emissions. With increasing in the concentration of Tm^{3+} upto 0.6 mol% (G6), the intensity of red emission increased slightly, while the blue emission intensity increases to a larger extent when compared with that of red emission. The results obtained provide useful information for choice of Tm and Yb concentration as well as for modelling and optimising the performance of upconversion lasers based Tm^{3+}/Yb^{3+} codoped lead bismuth gallium borate glasses. Also, these glasses offer the advantage of high chemical stability; they can remain as long as six months in the laboratory atmosphere without visible signs of deterioration, crystallization or hygroscopie.

V. REFERENCES

[1] S.Q. Man, E.Y.B. Pun, P.S. Chung, Appl. Phys. Lett. 77 (2000) 483.

[2] A.S. Oliverira, M.T. De Araujo, A.S. Gouveia Neto, A.S.B. Sombra, J.A. Medeiros Nneto, N. Aranha, J. Appl. Phys. 83 (1998) 604.

[3] L.H. Huang, X.R. Liu, W. Xu, B.J. Chen, J.L. Lin, J. Appl. Phys. 90 (2001) 5550.

[4] S. Xu, Z. Yang, J. Zhang, G. Wang, S. Dai, L. Hu, Z. Jiang, Chem. Phys. Lett. 385 (2004) 263.

[5] Q.H. Nie, C. Jiang, X.S. Wang, T.F. Xu, H.Q. Li, Mater. Res. Bull. 41 (2006) 1496.

[6] X. Shen, Q.H. Nie, T.F. Xu, Y. Gao, Spectrochim. Acta Part A 61 (2005) 2827.

[7] S.-Q. Xu, J.-J. Zhang, G.-N. Wang, S.-X. Dai, L.-L. Hu, Z.-H. Jiang, Chin. Phys. Lett. 21 (5) (2004) 927.

[8] X. Zhang, J.P. Jouart, G. Mary, J. Phys.: Condens. Matter 10 (1998) 493.

[9] A. Brenier, L.C. Courrol, C. Pedrini, C. Madej, G. Boulon, Opt.Mater. 3 (1994) 25.

[10] M. Yamazaki, K. Kojima, Solid State Commun. 130 (2004) 637.

[11] G.M. Salley, R. Valiente, H.U. Guedel, J. Lumin. 94 (2001) 305.

[12] A.S. Gouveia-Neto, E.B. da Costa, L.A. Bueno, S.J.L. Ribeiro, Y. Messaddeq, J. Lumin. 116 (2006) 52.

[13] X.B. Chen, W.M. Du, N. Sawanobori, G.Y. Zhang, Z.F. Song, Opt. Commun. 181 (2000) 171.

[14] S.Q. Xu, J.J. Zhang, G.N.Wang, S.X. Dai, L.L. Hu, Z.H. Jiang, Chin. Phys. Lett. 21 (2004) 927.

[15] Virender Kundu, R.L. Dhiman, A.S. Maan and D.R. Goyal *Advances in Condensed Matter Physics*, Volume 2008, Article ID 937054, 7 pages.

[16] M.C.S. Reddy, B. Appa Rao, M.G. Brik, A. Prabhakar Reddy, P. RaghavaRao, C.K. Jayasankar and N. Veeraiah *Applied Physics B*108(2) (2012) 455-461.

[17] Xiang Shen, QiuHua Nie, TieFeng Xu and Yuan Gao *Spectrochimica Acta Part A* 61 (2005) 2827–2831

[18] G. Lakshminarayana, Mengfe iMao, RongYang, J.R.Qiu and M.G.Brik *Physica B* 404 (2009) 3348–3355

[19] Shilong Zhao, Shiqing Xu, Degang Deng, Huanping Wang, Lihui Huang and Xianping Fan *Chemical Physics Letters* 494 (2010) 202–205

[20] F. Urbach *Phys. Rev.* 92 (1953) 1324.

[21] D. Redfield *Phys. Rev.* 130 (1963) 916.

[22] D.L. Dexter *Phys. Rev. Lett.* 19 (1967) 1383.

[23] I.A. Weinstein, A.F. Zatsepin and V.S. Kortov *J. Non-Cryst. Solids* 279 (2001) 77.

[24] J.M. Stevels *Verves Refract.* 2 (1948) 1.

[25] R.D. Sheibani and C.A. Hogarth *J. Mater. Sci.* 26 (1991) 429.

[26] K. Li, S. Fan, L. Zhang, Q. Zhang, J. Zhang and L. Hu *J. Non-Cryst. Solids* 357 (2010) 2417–2420.

[27] P.R. Watekar, S. Ju and W.T. Han *J. Non-Cryst. Solids* 354 (2008) 1453.

[28] G. Ozen, A. Aydinli, S. Cenk and A. Sennarogle *J. Lumin.* 101 (2003) 293.

[29] N. Sooraj Hussain, N. Ali, A.G. Dias, M.A. Lopes, J.D. Santos and S. Buddhudu *Thin Solid Films* 515 (2006) 318 – 325.

[30] A. Veerabhadra Rao, C. Laxmikanth, B. Appa Rao and N. Veeraiah *J. Phys. Chem. Solids* 67 (2006) 2263.

[31] J.S.De. Andrade, A.G. Pinheiro, I.F. Vasconcelos, J.M. Sasaki, J.A.C.D.E. Paiva, M.A. Valente and A.S.B. Sombra *J. Phys. Condens. Matter* 11 (1999) 4415.

[32] W.H. Hung, C.S. Ray and D.E. Ray *J. Am. Ceram. Soc.* 77 (1994) 1071

[33] Meisong Liao, Lili Hu, Yongzheng Fang, Junjie Zhang, Hongtao Sun, Shiqing Xu, Liyan Zhang, *Spectrochimica Acta Part A* 68 (2007) 531–535

[34] Meisong Liao, Shunguang Li, Hongtao Sun, Yongzheng Fang, Lili Hu, Junjie Zhang, *Materials Letters* 60 (2006) 1783–1785

[35] D.C. Yeh, W.A. Sibley and M.Suscavage *J. Appl. Phys.* 62 (1987) 266.

[36] Hai Lin, Ke Liu, Lin Lin, Yanyan Hou, Dianlai Yang, Tiecheng Ma, Edwin Yun Bun Pun, Qingda An, Jiayou Yu and Setsuhisa Tanabe *Spectrochimica Acta Part A* 65 (2006) 702-707.

[37] R. Visocekas, T. Ceva, T. Marti, F. Leaucheux and M.C. Robert *Phys. Status Solidi A* 35 (1976) 315.

[38] Octavio Meza, E.G. Villabona-Leal, L.A. Diaz-Torres, H. Desirena, J.L. Rodriguez-Lopez and Elias Perez *J. of Phy. Che. A* 118 (2014) 1390-1396.

[39] M. Ilhan, R. Samur, H. Demirer and F. Mindivan *Metalurgija* 54 (2012) 2 407-410.